

## Highly Resistive InP Embedded InGaAsP/InP Lasers Entirely Grown by Hydride VPE

Yoshitake KATO, Kenichi KASAHARA, Shigeo SUGOU, Tomoo YANASE and Naoya HENMI

Opto-Electronics Res. Labs., NEC Corporation

4-1-1 Miyazaki, Miyamae-ku, Kawasaki, Kanagawa 213, Japan

1.3 $\mu$ m InGaAsP/InP buried heterostructure laser diodes were grown entirely by hydride vapor phase epitaxy. For reducing the parasitic capacitance, selective growth technique of an Fe-doped InP embedding layer was adopted. It was found that resistance for the embedding layers depends on the channel structure. Current blocking effect was enhanced by increasing the channel width. At 20°C, the threshold current and the external differential quantum efficiency were 23mA and 17%/facet, respectively. 3dB-down roll-off frequency of over 10GHz was observed with the small-signal response. Furthermore, 5Gb/s RZ random pulse modulation was successfully demonstrated.

### 1. Introduction

InGaAsP/InP buried heterostructure (BH) laser diodes with a Fe-doped InP current blocking layer are attractive high-speed light sources, because of their low parasitic capacitance<sup>1</sup>. Moreover, Highly resistive InP embedded BH lasers are suitable for mass production due to simple structure and easy fabrication.

Hydride vapor phase epitaxy (VPE) for Fe-doped InP has such advantages as that 1) a smaller concentration of Fe is required in attaining high resistivity, because purer InP can be grown and 2) totally selective embedding growth with a flat surface is possible. VPE for double heterostructure (DH) wafers has advantages over liquid phase epitaxy in regard to productivity, controllability and uniformity. DH wafers, grown by hydride VPE with a multi-growth-chamber<sup>2</sup>, show highly uniform laser characteristics<sup>3</sup> and high reliability<sup>4</sup>. Entirely VPE grown BH lasers with current blocking layers consisting of Fe-doped InP are promising from the view points of laser characteristics and mass production.

This paper reports electrical properties measured for Fe-doped selectively embedding layers. It was found that the embedding layer resistance depends on the channel structure. The current blocking effect of the Fe-doped InP embedding layers has been enhanced by increasing the channel width.

Double heterostructure wafers were grown by hydride VPE. Then, Fe-doped InP current blocking layers were fabricated by selective VPE growth. The laser properties and the high frequency response in the BH lasers are obtained.

### 2. The growth and the electrical property of Fe-doped InP

The hydride VPE apparatus used for Fe-doped InP growth was described previously<sup>5</sup>. An In source containing Fe metal (an Fe/In source) and a pure In source were set separately in the source region. Compared to the previous report, the length of the Fe/In source region was increased to ensure the sufficient reaction time between the supplied HCl and the Fe/In source. The doped Fe concentration, evaluated by SIMS measurements, was proportional to the 2nd power of

the initial HCl partial pressure over the Fe/In source, as shown in Fig. 1. This is in agreement with thermodynamic calculations. It is shown that the reaction time between Fe and HCl is sufficient to achieve thermodynamic equilibrium in the present experiment. Fe concentration could be controlled simply by initial HCl partial pressure. Superior controllability for Fe doping was obtained with the present scheme.

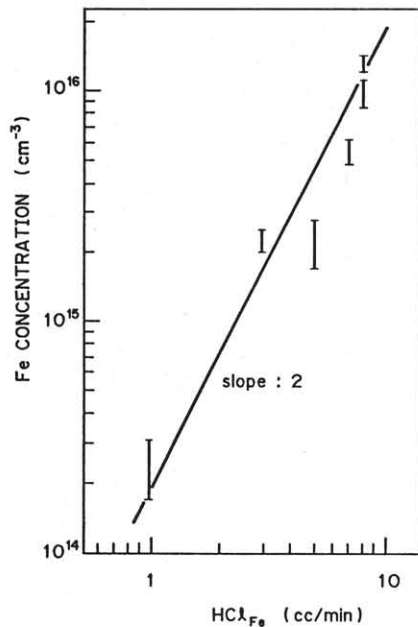


Fig.1, The dependence of the doped Fe concentration on HCl flow rate supplied over Fe/In source. Fe concentrations were evaluated by SIMS.

Figure 2 shows the resistivity of Fe-doped InP layers as a function of doped Fe concentrations evaluated by SIMS measurements. In order to investigate electrical properties, samples with 0.5mm $\phi$  AuGe/Ni electrodes deposited on them were fabricated from Fe-doped InP layers grown on n-InP substrates. The layer resistivity was estimated from the ohmic region of the current-voltage characteristics. This characteristic dependence of resistivity on Fe concentration was supported by a calculation taking into account the neutrality condition of the minority carriers. The background carrier

concentrations were 7.2–8.5 × 10<sup>14</sup> cm<sup>-3</sup>. The maximum resistivity obtained was 3.2 × 10<sup>8</sup> ohm-cm. SIMS depth profiles show that the Fe concentration was uniform along the epi-layer depth and changed rapidly at the interface between the epi-layer and the substrate. The abrupt change in the Fe concentration is important for device applications.

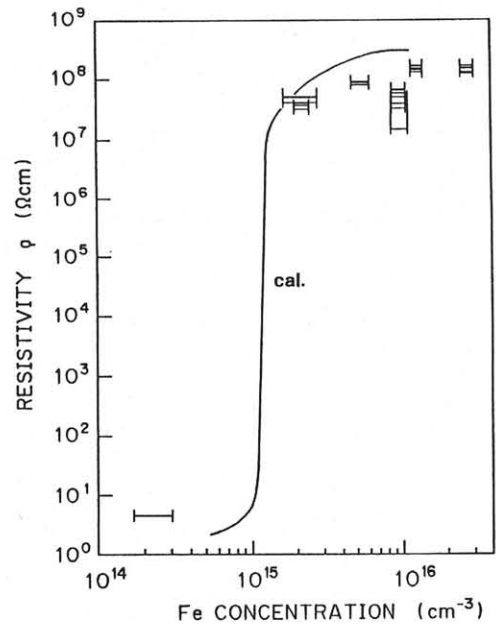


Fig.2, Fe-doped InP layer resistivity as a function of doped Fe concentration. The maximum resistivity obtained was 3.2 × 10<sup>8</sup> ohm-cm.

The electrical properties of Fe-doped InP embedding layers were measured. A cross sectional view of a sample is shown in Fig. 3(a). The samples were fabricated as follows. First, Fe-doped InP layers (~10<sup>8</sup> ohm-cm) were grown on an n-InP substrate. Next, chemical etching was performed on the wafer to form channels using SiO<sub>2</sub> masks. Then, Fe-doped InP was selectively grown in the channels. Without removing SiO<sub>2</sub> masks, a Ti/Pt/Au electrode was evaporated over the wafer surface and the samples were annealed at 430°C. Currents passing through the embedding layer with an applied voltage of 1V (I<sub>L</sub>) were measured for the samples with dif-

ferent groove shapes and width. It was found that  $I_L$  depends on the groove shape, and especially on the channel width.  $I_L$  tended to decrease with increasing channel width. For example, at  $5\mu\text{m}$  channel width,  $I_L$  included a few-tens of mA range. This  $I_L$  value was greater than the value expected from Fig. 2. At  $20\mu\text{m}$  channel width, however, the total resistance for the embedding layer increased, and the  $I_L$  value was less than about 1mA, as shown in Fig. 3(b).

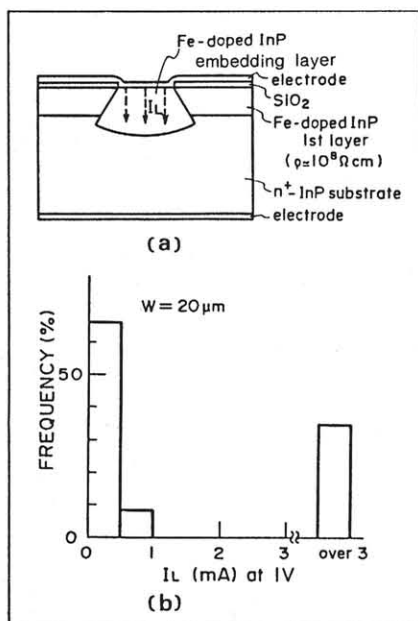


Fig.3, The electrical property for Fe-doped InP embedding layers.  $I_L$  denotes the passing current through the embedding layer. (a) Sample structure. (b)  $I_L$  histogram.

The change of the embedding layer resistance with increasing channel width was conjectured to be due to the change of the growth mechanism in the channel grooves. It is possible that the resistivity of the Fe-doped InP epi-layer grown on a certain crystal plane is lower than for other planes. In order to confirm this possibility, electrical properties for Fe-doped InP layers grown on different substrate planes were measured. It was found that the resistivity is lower for a (111)A plane substrate, which is iden-

tical to the crystal plane of the side wall of the present grooves, than for (100). The resistivity of an epi-layer on a (111)A substrate was  $5.6-21 \times 10^3$  ohm-cm. Therefore, the improvement in the current blocking effect by increasing channel width can be explained as follows: the growth on a (111)A plane is suppressed and the growth on a (100) plane occurs preferentially, which results in the high resistance.

### 3. BH lasers entirely grown by VPE

DH wafers were grown by hydride VPE on the (100)-[110]  $2^\circ$  off n-InP substrates. The growth temperature was  $690^\circ\text{C}$ . The DH wafer consisted of an n-InP buffer layer, a  $1.3\mu\text{m}$  InGaAsP active layer, a p-InP cladding layer and a p-InGaAsP cap layer. Then, double channels were formed by wet chemical etching, using an  $\text{SiO}_2$  mask. Channel width was  $20\mu\text{m}$ . In the second growth, Fe-doped InP was selectively embedded with hydride VPE in the channels at  $600^\circ\text{C}$  growth temperature. The schematic cross section of the device is shown in Fig. 4. The laser was p-side up mounted.

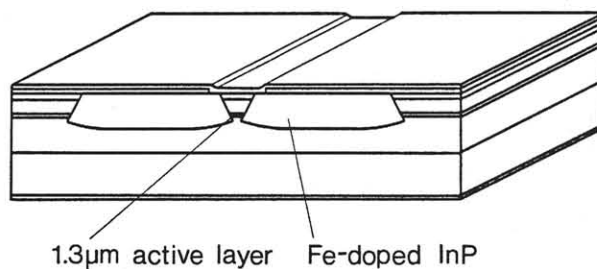


Fig.4, Structure for highly resistive InP embedded  $1.3\mu\text{m}$  InGaAsP/InP buried heterostructure lasers.

To evaluate threshold current density ( $J_{th}$ ),  $\text{SiO}_2$  stripe lasers with different stripe width, were fabricated by using the same wafer. For  $46\mu\text{m}$  stripe width, the  $J_{th}$  value was  $2.2\text{kA}/\text{cm}^2$ . The net  $J_{th}$  value with eliminating the influence of current spreading was  $1.7\text{kA}/\text{cm}^2$ .

Figure 5 shows light-output versus CW

drive current (L/I) curves. At 20°C, the threshold current and the external differential quantum efficiency were 23mA and 17%/facet, respectively. The CW threshold current increases with temperature proportional to  $\exp(T/T_0)$ , with  $T_0=61K$  in the 20°C–50°C range.

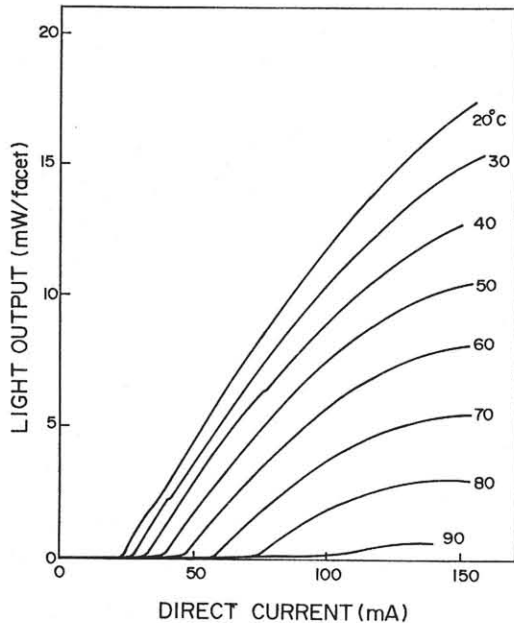


Fig.5, CW light output versus drive current (L/I) characteristics for 1.3µm InGaAsP/InP lasers entirely grown by hydride VPE.

Small-signal responses with a sinusoidal modulation for the BH lasers, at several CW bias levels, were measured. 3dB-down roll-off frequency of over 10GHz was observed. Figure 6 shows optical response for 5Gb/s RZ random pulse modulation. Nice eye opening has been realized. High frequency response could be confirmed in the lasers embedded with Fe-doped InP.

#### 4. Conclusions

Fe-doped semi-insulating InP embedded InGaAsP/InP lasers were fabricated entirely by hydride VPE. With Fe-doped highly resistive embedding layers, it was found that the resistance for the embedding layers depends on channel structure. Current blocking effect increased as the channel became wider.

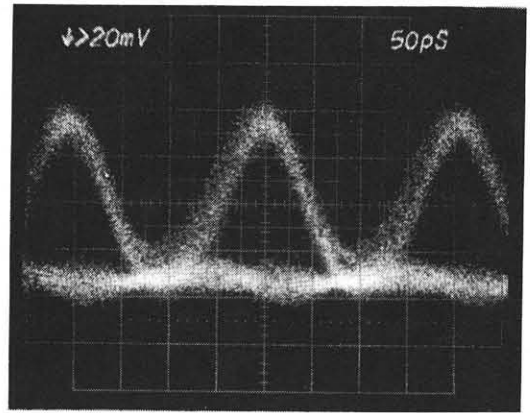


Fig.6, Optical response for 5Gb/s RZ random pulse modulation.

At 20°C CW operation, the threshold current and external differential quantum efficiency were 23mA and 17%/facet, respectively. 3dB-down roll-off frequency of over 10GHz was obtained. Furthermore, 5Gb/s RZ modulation was successfully demonstrated.

The authors wish to acknowledge A.Usui, R.Lang, H.Watanabe, M.Ogawa, K.Kobayasi and K.Minemura for fruitful discussions and encouragement. The authors also thank E.Saito for laser processing.

#### Reference

- 1) G.Eisenstein, U.Koren, R.S.Tucker, B.L.Kasper, A.H.Gnauck, and P.K.Tien, *Appl. Phys. Lett.*, **45** (1984) 311.
- 2) T.Mizutani, M.Yoshida, A.Usui, H.Watanabe, T.Yuasa, and I.Hayashi, *Jpn. J. Appl. Phys.* **19** (1980) L113.
- 3) T.Yanase, S.Sugou, Y.Sasaki, Y.Kato, K.Nishi, and T.Murakami, *OEC-86 Technical Digest*, 1986, Tokyo, pp.208.
- 4) S.Sugou, H.Nishimoto, M.Kitamura, I.Mito, and Y.Yanase, *Electron. Lett.*, **21** (1985) 1154.
- 5) Y.Kato, A.Usui, T.Kamejima, S.Sugou, and K.Kasahara, *Int. Symp. GaAs and Related Compounds*, USA, 1986, pp.395.